Proceedings World Geothermal Congress 2020+1
Reykjavik, Iceland, April - October 2021

Modelling and Stability Analysis of Geothermal Power Plants

Luis A. Aguirre

LaGeo S.A. de C.V., 15 Avenida Sur, Colonia Utila. Santa Tecla, La Libertad. El Salvador

aguirrel@lageo.com.sv

Keywords: Geothermal Power Plants, Rotor Stability

ABSTRACT

Power system stability can be defined as the property of a power system that enables it to remain in a state of operating equilibrium under normal operating conditions and to regain an acceptable state of equilibrium after being subjected to a disturbance. There are different forms of power systems stability, but this project is focused on rotor angle stability.

Rotor angle stability is the ability of interconnected synchronous machines of a power system to remain in synchronism. For convenience in analysis and for gaining useful insight into de nature of stability problems, rotor angle stability phenomena are characterised in two categories:

- Small-signal stability is the ability of the power system to maintain synchronism under small disturbances like the variations in load and generation.
- Transient stability is the ability of the power system to maintain synchronism when subjected to a severe transient disturbance like short-circuits of different types.

Energy consumption in El Salvador has had an increase of 199.8% since 1995, caused by the industrial and commercial growing in the country and the increase in the population. The peak power demand in 1995 was 591.7 MW, compared with peak power demand in 2017 of 1081 MW. This power consumption increase required the construction of new power plants to satisfy the demand (SIGET, 2017).

Since 2007, Berlin Geothermal power plant has had an installed capacity increase of 46 MW with the installation of two new generators. There are also new plans about the installation of two more generators around 2020, with a total capacity of 35 MW. This growing will cause changes in power flow and dynamics characteristic of the power system that has to be taken into account for the development of geothermal energy in El Salvador.

A dynamic simulation model of Berlin geothermal power plant in El Salvador is built with MATLAB/Simulink with the objective of doing a dynamic study of the system taking into account the future generators. This study enables us to analyse the dynamic behaviour of the power plant with small and severe disturbances in the power system.

The dynamic study takes into account the most important parts of the geothermal power plant like Turbine, Governor, Generator, Excitation system, transformers and transmission lines to get a good approximation of the systems and acceptable results.

1. INTRODUCTION

Geothermal energy is one of the most important forms of renewable energy and it has several uses around the world. In 2009, electricity was produced from geothermal energy in 24 countries, increasing by 20% from 2004 to 2009 (Fridleifsson and Haraldsson, 2011). The countries with the highest geothermal installed capacity in MW were USA (3,093 MW), Philippines (1,197 MW), Indonesia (1,197 MW), Mexico (958 MW) and Italy (843 MW). In terms of the percentage of the total electricity production, the top five countries were Iceland (25%), El Salvador (25%), Kenya (17%), Philippines (17%) and Costa Rica (12%) (Bertani, 2010)

There are two geothermal fields in El Salvador that have operating power plants: Ahuachapán and Berlin. Their combined installed capacity is 204.4 MW.

Ahuachapán geothermal power plant consists of three units, two of them are condensing units, single flash cycle (SF) 30 MW each, and one condensing unit, double flash cycle (DF) of 35 MW. Berlin Geothermal power plant consists of four units, three of them, unit 1 and unit 2 of 28 MW each and unit 3 of 44 MW, are SF and the other one is an Organic Rankine cycle (ORC) of 9.2 MW (Guidos and Burgos, 2012).

Berlin Geothermal Power plant (CGB), the one object of study in this project, has as projections of new development, the construction of one condensing unit SF of 28 MW and one ORC of 7 MW as future projects. The new power generation developments at CGB cause changes in power flow and dynamics characteristic of the electrical system in El Salvador, but specially affects the dynamics behaviour of the existing units.

The purpose of this document is to make a detailed dynamic model of the power plant together with the surrounding power grid, to be able to perform the dynamic studies of the power plant, taking into account the existing and future units. The dynamic simulation model of CGB performs with SymPowerSystems, a package of MATLAB/Simulink, that is a design tool that allows building models that simulate power systems.

For the model building, database of the transmission line company in El Salvador has been utilised (ETESAL, 2015), the database of the electrical market administrator in El Salvador (UT, 2013), manufacturer data sheets and information of the owner of CGB (LaGeo S.A. de C.V.).

2. EL SALVADOR 115 KV ELECTRICAL SYSTEM

The generation distribution in Salvadorian electrical system is composed of different kinds of power plants, like Hydroelectric (34.3%), Geothermal (24.5%), Fuel (36.3%) and Biomass (2%). The rest of the energetic matrix is covered with imports. In 2011, the total installed capacity of electrical power in El Salvador was 1,477.2 MW, with an annual increase of 1.1%, respect to 2010 because of the start of operation for generators installed in Chaparrastique sugar mill, with a capacity of 16 MW (SIGET, 2017).

Figure 1: Electrical system in El Salvador

El Salvador covers an area of 21.000 km², and its national transmission system is composed of 38 lines of 115 kV, which have a total length of 1072.49 km. Otherwise, there are two lines of 230 KV that interconnect the transmission system of El Salvador with the transmission system of Guatemala and Honduras. The length of the line to Guatemala is 14.6 km and 92.9 km to Honduras. There are 23 substations with a transformation capacity of 2,386.7 MVA. Figure 1 shows the one-line diagram of the electrical system in El Salvador

The maximum demand of the electrical system during 2011 was 962 MW, with an annual grown of 1.5% respect to 2010. There is a small amount of small hydroelectric generators connected directly to the distribution system at 46 KV with an installed capacity of 26.3 MW and an available capacity of 24.1 MW.

3. POWER SYSTEM STABILITY

Power system stability is the ability of an electric power system, for a given initial operation condition, to regain a state of operating equilibrium after being subjected to a physical disturbance, with most system variables bounded so that practically the entire system remains intact. Theory of section 3 has been taken to (Kundur et al., 2003) and (Kundur, 1994).

The previous definition applies to an interconnected power system as a whole. Often, however, the stability of a particular generator or group of generators is also of interest. A remote generator may lose stability (synchronism) without cascading instability of the main system.

Power systems are subjected to a wide range of small and large disturbances. Small disturbances in the form of load changes occur continually; the system must be able to adjust to the changing condition and operate satisfactorily. It must also be able to survive numerous disturbances of a severe nature, such as a short circuit (SC) on a transmission line or loss of a large generator.

The response of the power system to a disturbance involves much of the equipment. For example, a fault on a critical element followed by its isolation by a protective relay will cause variations in power flows, network bus voltages and machine rotor speeds; the voltage variations will actuate both generators and transmission network, voltage regulators; the generator speed variations will actuate prime

movers governors and the voltage and frequency variations will affect the system loads to varying degrees depending on their individual characteristics. Besides, devices used to protect individual equipment may respond to variations in system variables and cause tripping of the equipment, thereby weakening the system and possibly leading to system instability.

If following a disturbance, the power system is stable, it will reach a new equilibrium state with the system integrity preserved i.e., with practically all generators and loads connected through a single contiguous transmission system. Power systems are continually experiencing fluctuations of small magnitudes. However, for assessing stability when subjected to a specific disturbance, it is usually valid to assume that the system is initially in a true steady-state operating condition.

3.1. Power Versus Angle Relationship

The relationship between interchange power and angular position of the rotors of synchronous machines is an important characteristic that has a bearing on power system stability. This relationship is nonlinear. To illustrate this, we will consider a synchronous generator connected to a motor by a transmission line having an inductive reactance X_L.

The power transferred from the generator to the motor is a function of angular separation (δ) between the rotors of the two machines. This angular separation is due to three components: generator internal angle, the angular difference between the terminal voltage of the generator and motor (caused by transmission line impedance) and internal angle of the motor. The power transferred from the generator to the motor is given by

$$P = \frac{E_G E_M}{X_T} sin\delta \tag{1}$$

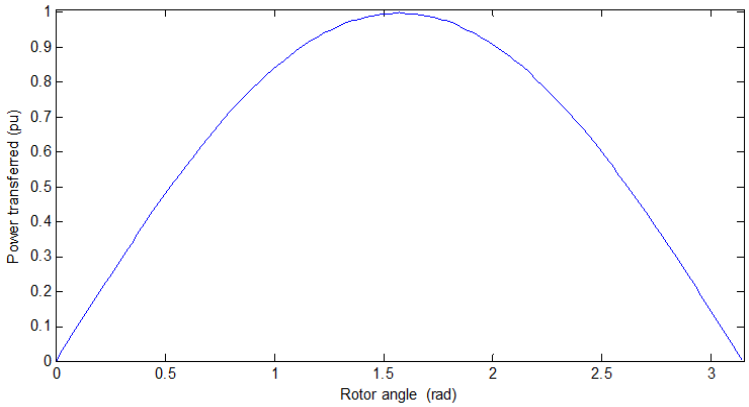

Figure 2: Power-angle curve

Where subscript G and M refers to generator and motor respectively and $X_T = X_G + X_L + X_M$. The corresponding power versus angle relationship is plotted in figure 2. As the angle is increased, the power transfer increases up to a maximum. After a certain angle, nominally 90°, a further increase in angle results in a decrease in power transferred. Angular separation (δ) for a particular generator is normally referred to as rotor angle or load angle.

3.2. Rotor Angle Stability

Rotor angle stability is the ability of synchronous machines of an interconnected power system to remain in synchronism after being subjected to a disturbance. It depends on the ability to maintain/restore equilibrium between electromagnetic torque and mechanical torque of each synchronous machine in the system. The instability that may result occurs in the form of increasing angular swings of some generators leading to their loss of synchronism with other generators.

Rotor angle stability problem involves the study of the electromechanical oscillations inherent in power systems. A fundamental factor in this problem is the manner in which the power output of synchronous machines varies as their rotor angle change. Under steady state conditions, there is equilibrium between the input mechanical torque and the output electromagnetic torque of each generator, and the speed remains constant. If the system is perturbed, this equilibrium is upset, resulting in acceleration or deceleration of the rotors of the machines according to the laws of motion of a rotating body. If one generator temporarily runs faster than another, the angular position of its rotor relative to that of the slower machine will advance. The resulting angular difference transfers part of the load from the slow machine to the fast machine, depending on the power-angle relationship. This tends to reduce the speed difference and hence the angular separation.

The change in electromagnetic torque of a synchronous machine following a perturbation can be resolved into two components:

- Synchronizing torque component, in phase with rotor angle deviation.
- Damping torque component, in phase with the speed deviation.

System stability depends on the existence of both components of torque for each of the synchronous generators. Lack of synchronizing torque results in aperiodic or non-oscillatory instability, lack of damping torque results in oscillatory instability. For convenience in analysis, it is useful to characterize rotor angle stability in terms of the following two subcategories:

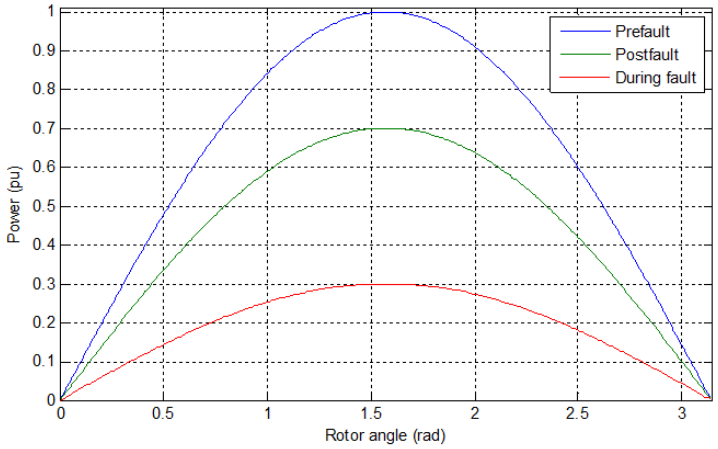

Figure 3: Power-angle curves during a fault

- Small Disturbance (or small signal) rotor angle stability, is concerned with the ability of the power system to maintain synchronism under small disturbances. The disturbances are considered to be sufficiently small that linearization of system equations is permissible for purposes of analysis. Small-disturbance stability depends on the initial operating state of the system. The instability that may result can be of two forms: increase in rotor angle through a non-oscillatory or aperiodic mode due to lack of synchronizing torque or rotor oscillations of increasing amplitude due to lack of sufficient damping torque.
- Large disturbance rotor angle stability or transient stability, as it is commonly referred to, is concerned with the ability of the power system to maintain synchronism when subjected to a severe disturbance, such as a short circuit on a transmission line. The resulting system response involves larges excursions of generator rotor angles and is influenced by the nonlinear power-angle relationship. Transient stability depends on both the initial operating state of the system and the severity of the disturbance. Instability is usually in the form of aperiodic angular separation due to insufficient synchronizing torque, manifesting as first swing instability.

Small signal stability and transient stability are categorized as short-term phenomena, with a time frame of interest on the order of 10-20 seconds following a disturbance. During transient stability phenomena, there are changes in the operation point of the power-angle relationship curve because of changes in reactance caused by loss of transmission lines or generators. Figure 3 shows typical power-angle relationship plot for the three-network conditions; pre-fault, post-fault and during the fault.

3.3. Eigenvalues and Stability

For power system stability studies, the characteristic of a system can be determined by the analysis of the eigenvalues of the linearized system. The eigenvalues of a matrix are given by the values of the scalar parameter λ for which there exist non-trivial solutions (i.e., other than ϕ=0) to the equation

$$A\phi = \lambda\phi \tag{2}$$

Where

A is the state nxn matrix (real for a physical system such as a power system)

ϕ is an nx1 vector

To find the eigenvalues, equation 2 may be written in the form

$$(A - \lambda I)\phi = 0 \tag{3}$$

For a non-trivial solution

$$\det(A - \lambda I) = 0 \tag{4}$$

Expansion of the determinant gives the characteristic equation. The n solutions of $\lambda=\lambda_1, \lambda_2, \ldots, \lambda_n$ are the eigenvalues of A. The eigenvalues may be real or complex. If A is real, complex eigenvalues always occur in conjugate pairs (Kundur, 1994).

The time dependent characteristic of a mode corresponding to an eigenvalue λ_i is given by $e^{\lambda_i t}$. A real eigenvalue corresponds to a non-oscillatory mode. A negative real eigenvalue represents a decaying mode. A positive real eigenvalue represents aperiodic instability. Complex eigenvalues occur in conjugate pairs, and each pair corresponds to an oscillatory mode. Thus, for a complex pair of eigenvalues:

$$\lambda = \sigma \pm j\omega \tag{5}$$

The real component of the eigenvalues gives the damping and the imaginary component gives the frequency of oscillation. A negative real part represents a damped oscillation (stable system) whereas a positive real part represents oscillation of increasing amplitude (unstable system). The frequency of oscillation is given by:

$$f = \frac{\omega}{2\pi} \tag{6}$$

This represents the actual or damped frequency. The damping ratio determines the rate of decay of the amplitude of the oscillation and is given by:

$$\zeta = \frac{-\sigma}{\sqrt{\sigma^2 + \omega^2}} \tag{7}$$

The damping ratio ζ determines the rate of decay of the amplitude of the oscillation; it means that amplitude decays to 37% of initial amplitude in $1/|\sigma|$ seconds or in $1/2\pi\zeta$ cycles of oscillation.

3.4. Prony Analysis

Eigenvalue calculation is very complex for a power system that has non-linear components and where not all the information to develop the linearization is available. This is the case for the analysis object of the present project. In this case, Prony analysis is used for eigenvalues calculation.

Prony analysis estimate directly the frequency, damping, strength and relative phase of modal components presents in a given signal. Prony methods and their recent extensions are designed to directly estimate the eigenvalues λ_i (and eigenvectors) of a dynamic system by fitting a sum of complex damped sinusoids to evenly space sample (in time) values of the output described below (Hauer, Demeure, Scharf, 1990)

$$\hat{y}(t) = \sum_{i=1}^{Q} A_i e^{\sigma_i t} \cos(2\pi f_i t + \phi_i) \tag{8}$$

where

A_i is the amplitude of component i,

σ_i is the damping coefficient of component i (real part of eigenvalues)

ϕ_i is the phase of component i

f_i is the frequency of component i (imaginaries part of eigenvalues, $\omega i = 2\pi fi$)

Q: Total number of damped exponential components

For the Prony analysis in MATLAB, there have been used Prony Toolbox (Singh, 2003), which is a software tool built around MATLAB functions with a user-friendly graphical interface and containing all the necessary features to perform Prony Analysis.

With Prony Toolbox, it is possible to calculate the Eigenvalues and the poles of the system. Poles provide the angle of the eigenvector of the system, so it is possible to plot the eigenvector in a polar way, with amplitude A_i and angle ϕ_i for each generator group. Rotor speed signal has been used to perform Prony analysis.

Eigenvalues method for stability analysis can be applied just for small signal stability cases, where local stability conditions permit the linearization of the system. For the implementation of this method in cases with transient stability perturbations, like short circuits, the analysis is done during the time period that corresponds to small signal stability conditions, avoiding the first cycles of the oscillation, that are part of transient stability phenomena.

4. MODELING DESCRIPTION

Modelling of CGB required all the information and parameters of the components that are part of the system. Sometimes it is complicated to get this parameter and it is necessary to select typical values suggested by standard and references. The present model uses real parameters of the equipment nowadays installed and operating in the power plant, but in some particular cases because of lack of information or wrong data, a few parameters have been taken from typical values detailed by international standards. The detail of the modelling of each component will be described below.

4.1. Turbine

There are two kinds of turbines at CGB, Steam turbines for unit 1, unit 2 and unit 3, that works with an SF cycle and gas turbines for unit 4 that works with ORC. Both kinds of turbines are described below.

4.1.1 Steam Turbine

Steam turbines convert stored energy of high pressure and high temperature steam into rotating energy, which is, in turn, converted into electrical energy by the generator. The heat source for the boiler supplying the steam, in this case, is geothermal energy (Kundur, 1994).

Steam turbines consist of two or more turbine sections or cylinders coupled in series. Each turbine section has a set of moving blades attached to the rotor and a set of stationary vanes. The stationary vanes referred to as nozzle sections, form nozzles that accelerate the steam at high velocity. The kinetic energy of this high velocity steam is converted into shaft torque by the moving blades.

4.1.2 Gas Turbine

Gas turbine for this particular case is a Turbo-expander-generator group. A turbo-expander expands process fluid from the inlet pressure to the discharge pressure in two steps; first through variable inlet guide vanes (or nozzles assembly) and then through the radial wheel. As the accelerated process fluid moves from the inlet guide vanes to the expander wheel, kinetic energy is converted into useful mechanical energy. The mechanical energy drives the generator.

The nozzles are controlled by an electrically governed hydraulic amplifier, acting upon the assembly through an actuator rod. The actuator turns a low-level electrical signal from the Woodward governor to a rotary mechanical output, exerting an opening or a close force depending on the supplied oil pressure.

4.2 Governor

The prime mover governor systems provide a means of controlling power and frequency, a function commonly referred to as load-frequency control. Its basic function is to control speed and/or load. The governor receives speed signal input and controls the inlet valve/gate in steam turbines and the nozzles assembly for gas turbines, to regulate the power and frequency. Prime mover governor consists of two main components:

- Turbine controls, that receive all field control signals from the turbine-generator group and generate a control command. Turbine controls can be mechanical-hydraulic, electrohydraulic or digital electrohydraulic.
- Actuator, that receives the control command from the turbine control and executes a control action over the inlet valve/gate in steam turbines and the nozzles assembly for gas turbines. Actuators are normally hydraulic.

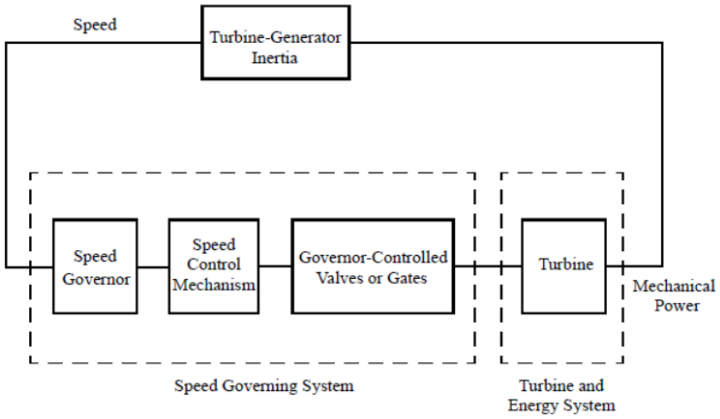

Figure 4: Speed governor and turbine in relationship to generator (Siemens, 2012)

Figure 4 shows a turbine and governor functional diagram and its relationship with generator Turbine-governor modelling in Simulink has been done by the transfer function of the TGOV1 Steam turbine governor, defined by PSSE governor blocks (SIEMENS, 2012).

4.3 Synchronous Generator

A synchronous generator consists of two essential elements: the field and the armature and the field winding are excited by direct current. When the rotor is driven by a turbine, the rotating magnetic field of the field winding induces alternating voltages in the three-phase armature winding of the stator. The frequency of the induced alternating voltages and of the resulting current that flows in the stator windings when a load is connected depends on the speed of the rotor. The frequency of the stator electrical variables is synchronized with the rotor mechanical speed: hence the designation Synchronous generator (Kundur, 1994).

When two or more synchronous machines are interconnected, the stator voltages and currents of all the machines must have the same frequency and the rotor mechanical speed of each is synchronized to this frequency. Therefore, the rotors of all interconnected synchronous machines must be in synchronism.

Stator and rotor field react with each other and an electromagnetic torque results from the tendency of the two fields to align themselves. This electromagnetic torque opposes rotation of the rotor so that mechanical torque must be applied by the prime mover to sustain rotation. The electrical torque output of the generator is changed only by changing the mechanical torque input by the turbine. An increase of mechanical torque input advances the rotor to a new position relative to the revolving magnetic field of the stator, a reduction of mechanical torque or power input will retard the rotor position. Under steady-state operating conditions, the

rotor field and the revolving field of the stator have the same speed. However, there is an angular separation between them depending on the electrical torque output of the generator.

Modelling of the generator in Simulink has been done with the block Synchronous machine pu Standard of SimPowerSystem library that represents electrical part of the synchronous generator by a sixth-order state space model and the mechanical part by the equations of motion described in (Kundur, 1994).

4.4 Excitation System Modelling

Excitation system provides direct current to the synchronous machine field winding. Additionally, the excitation system performs control and protective functions that are essentials to the satisfactory performance of the power system by controlling the field voltage and thereby the field current.

The general functional block diagram shown in Figure 5 indicates various synchronous machine excitation subsystems. These subsystems may include a terminal voltage transducer and load compensator, excitation control elements, an exciter, and, in some cases (but not our case of study), a power system stabilizer (IEEE 1992)

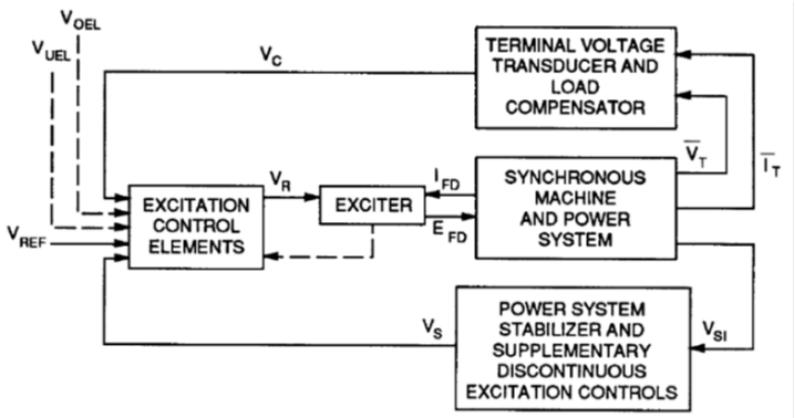

Figure 5: General Functional Block Diagram for Synchronous Machine Excitation Control System (IEEE, 1992)

Excitation system modelling in Simulink has been done by the transfer function of each particular model. Unit 1, Unit 2 and Unit 3 have an excitation system model AC1A, according to (IEEE, 1992). Unit 4 has a Basler Electric excitation system model DECS-200, which is not defined on (IEEE, 1992) but is expected to be part of the next revision of the standard.

4.5 Power Transformer

A power transformer is connected between the generator terminals and the transmission system and converts the voltage level of the generator to the transmission voltage level. Transformers in general, enable the utilization of different voltage levels across the system. From the viewpoint of efficiency and power-transfer capability, the transmission voltages have to be high to avoid losses.

Modelling of the transformer in Simulink has been done with the block Three-phase Transformer (Two Windings) of SimPowerSystem library that implements a three-phase transformer using three single-phase transformers.

4.6 Transmission Lines

Electrical power is transferred from generating stations to consumers through overhead lines, which are used for long distances in open country in the power transmission system. A transmission line is characterized by four parameters: series resistance R due to the conductor resistivity, shunt conductance G due to leakage currents between the phases and ground, series inductance L due to the magnetic field surrounding the conductors and shunt capacitance C due to the electric field between conductors. Shunt conductance represents losses due to leakage currents along insulators strings and corona. In power lines, its effect is small and usually neglected (Kundur, 1994).

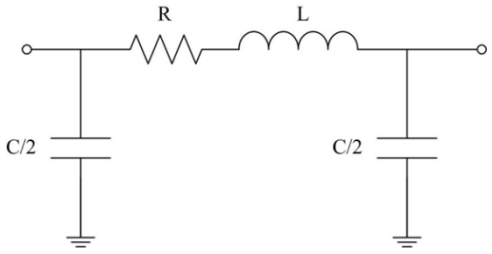

Figure 6: PI section representation for transmission lines.

The modelling of the transmission lines in Simulink has been done with the block *Three-phase PI Section Line* of SimPowerSystem library that implements a three-phase transmission line model with parameters lumped in a PI section as shown in figure 6. The line parameters R, L and C are specified as positive and zero sequence parameters that take into account the inductive and capacitive coupling between the three phase conductors as well as the ground parameters. This method of specifying line parameters assumes that the three phases are balanced. Using a single PI section model is appropriate for modelling short lines, that are defined as lines shorter that around 80 km by (Kundur, 1994).

4.7 Generating Unit Group Modelling.

CGB consists of three SF units (unit 1, unit 2 and unit 3) and one ORC unit (unit 4). There are one SF unit and one ORC unit that will be developed in the future and have been including on this project (unit 5 and unit 6 respectively). Unit 1, unit 2 and unit 5 have the same parameters, so, the simulation results for these units will be very similar. The same applies for unit 4 and unit 6, the only

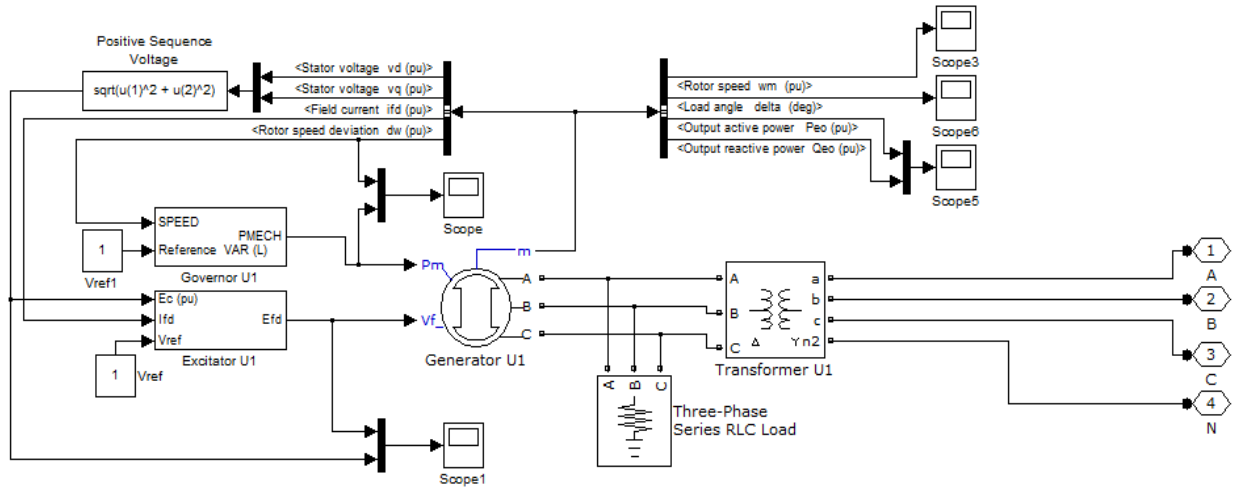

Figure 7: Generating unit group modelling in Simulink.

difference is the length of the internal transmission line for both units, but basically, the simulation results will be very similar for these units too.

Each generating unit group consists of Turbine, Governor, Generator, excitation system, and transformer; all of them are part of the stability analysis. Figure 7 shows the generating Unit 1 modelling in Simulink. It can be seen in the figure, the scope blocks for viewing of different parameters of the system. Each generating unit is a subsystem of CGB modelling described later.

4.8 CGB Modelling

Modelling of CGB include the 6 generating unit group described before and part of the 115-kV transmission system in the surroundings of the power plant. There have included too the two internal transmission line of unit 4 and unit 6 that connect both units with the main substation. There have been included 3 buses in the system, CGB bus, where 6 units are connected, 15 de Septiembre bus, where the infinite bus is connected and San Miguel bus, where a big load is connected.

There have been modelled different disturbances in the system, like short circuit and load changes, and there have been included the circuit breakers for transmission system too. Both, short circuits and circuit breakers are part of SimPowerSystem library. Table 1 details the disturbances to be modelled.

Infinite Bus has been modelled by the block Three-phase Source of SimPowerSystem library, which implements a balanced three-phase voltage source with internal R-L impedance. Block characteristic is defined by a short circuit level and X/R ratio. Figure 8 shows the complete system modelling in Simulink for case 1.

Tag	Description
Base case	No perturbations in the network
Case 1	3-phase SC line BER-15SEPT
Case 2	3-phase SC line BER-SM
Case 3	3-phase SC line 15SEPT-SM

TABLE 1: Disturbances detail for CGB analysis

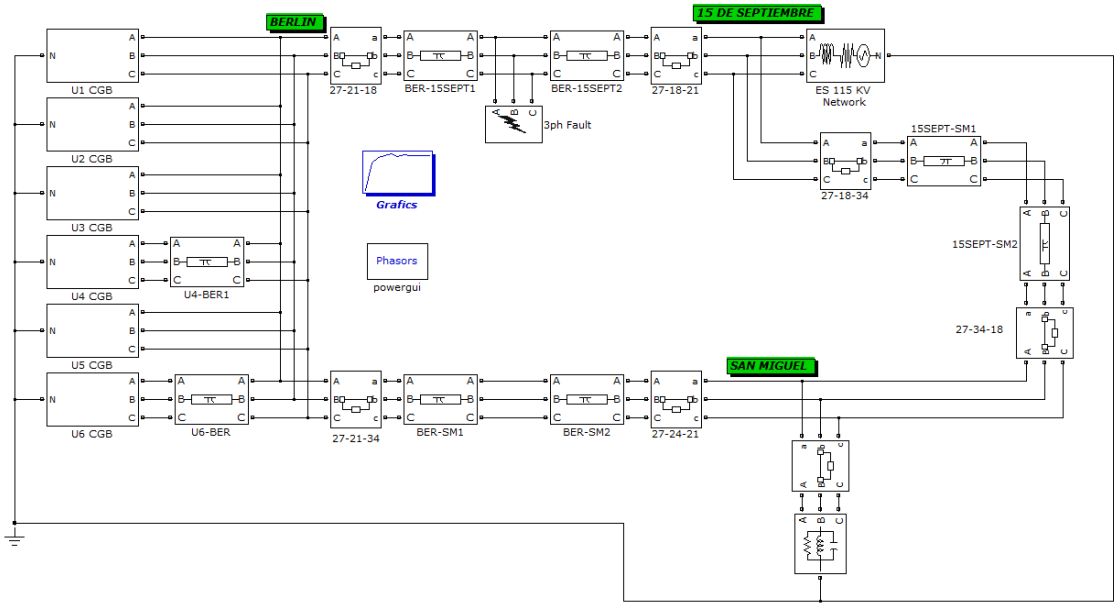

Figure 8: CGB Case 1 modelling in Simulink.

5. MODELING RESULTS

Simulation and modelling for the stability analysis in CGB have been realized based on the cases detailed in table 1. There will be show different plots of the most important variables of the system, as well as the calculation of eigenvalues and other important properties. For the base case, there will be the plots of rotor speed and load angle for each generator shown.

For case 1, case 2 and case 3 will be showed the plots of rotor speed, load angle and normalized eigenvectors for each unit. To normalize eigenvectors, the one with the highest magnitude is chosen as the reference and all of them, magnitude and angle, are divided by the reference eigenvector. Additionally, there have been calculated the eigenvalues, the damping ratio and the frequency of oscillation. The eigenvalues and eigenvectors have been calculated by the Prony analysis described in 3.4, using the rotor speed signal for the analysis.

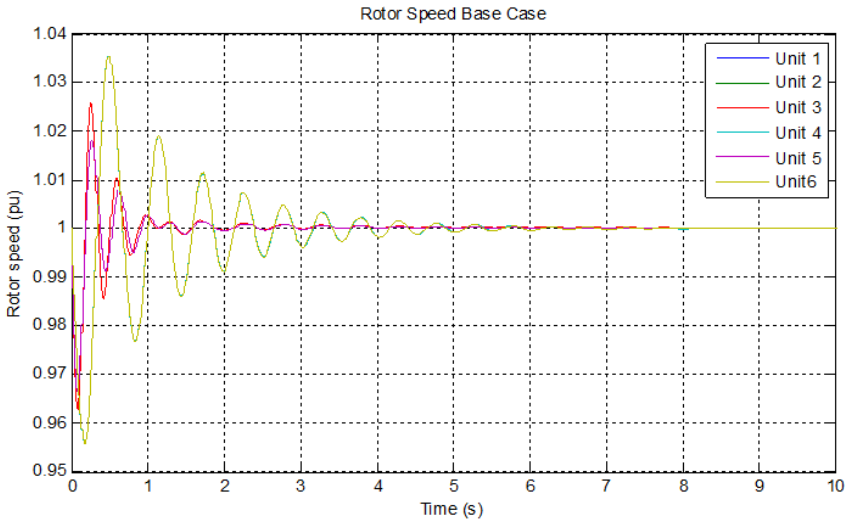

Figure 9: Rotor Speed CGB Base Case.

5.1 Base Case Simulation

The base case basically shows the behaviour of the system without any contingency. The simulation time is 75 seconds. During the first seconds of the simulation, the system is not in a stable state because of initial conditions. After approximately 40 seconds, the system becomes stable.

5.1.1 Rotor Speed

Figure 9 shows the rotor speed of CGB for the base case. Only the first 10 seconds have been shown because, after that time, the rotor speed becomes stable. The speed oscillations are just during the firsts 5 seconds because of the initial conditions.

5.1.2 Load angle.

Load angle shows the rotor angle of each machine respect to the load of the system. All load angles are lower than 90°, which indicate that power transfer has not reached the maximum value. Figure 10 shows the load angles for all generators.

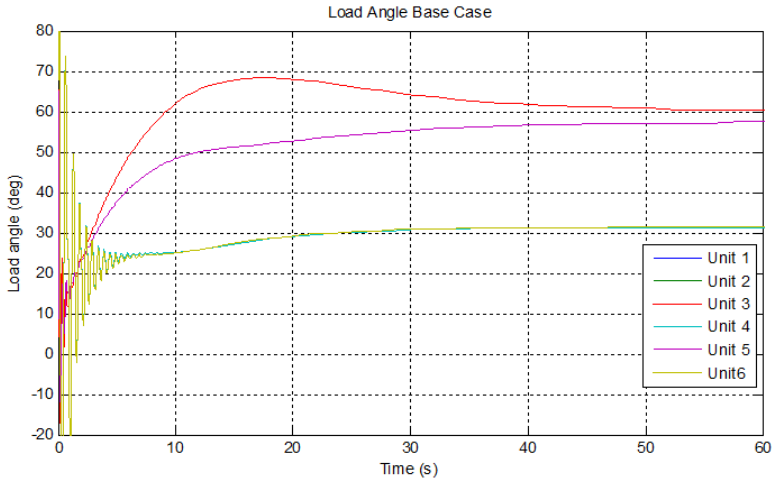

Figure 10: Load Angle CGB Base Case.

5.2 Case 1 Modelling

Case 1 modelling includes the same model of the base case but there have been added a 3-phase short circuit in the transmission line Berlin-15 de Septiembre. There have been including the operation of the circuit breakers in both ends of the line to clean the fault. The fault occurs at 75 seconds to let the systems been in steady state at the fault occurrence and the circuit breakers operate at 75.1 seconds. The total simulation time is 120 seconds, to let the system to reach a steady state again after the fault.

5.2.1 Rotor Speed

Figure 11 shows the rotor speed during the fault for case 1. It can be seen in the plots that the highest oscillations are for unit 4 and unit 6, with a deviation of 0.034 pu respect to nominal speed. It takes approximately 10 seconds after the fault occurrence to return to steady state.

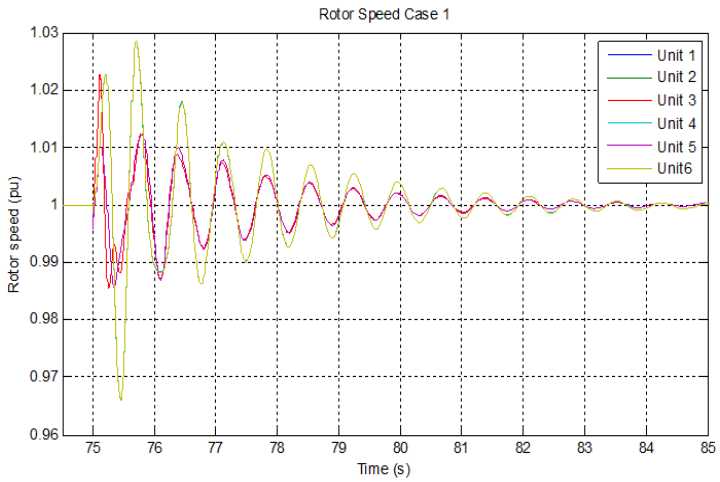

Figure 11: Rotor Speed CGB Case 1.

5.2.2 Load Angle

Figure 12 shows the load angle plots before, during and after the fault. Load angle change because of the network configuration change. Basically, the loss of transmission line cause changes in the impedances of the system, excitation system and governor of each generator try to re-accommodate the abnormal condition for each generator and this cause the load angle change.

For unit 1, unit 2 and unit 5 the load angle before the fault is 57.39° and after the fault, for steady state, it changes to 48.21°. For unit 3 the load angle change is for 60.22° to 52.82° and for units 4 and unit 6 there is practically no change, for 31.17° to 31.03°.

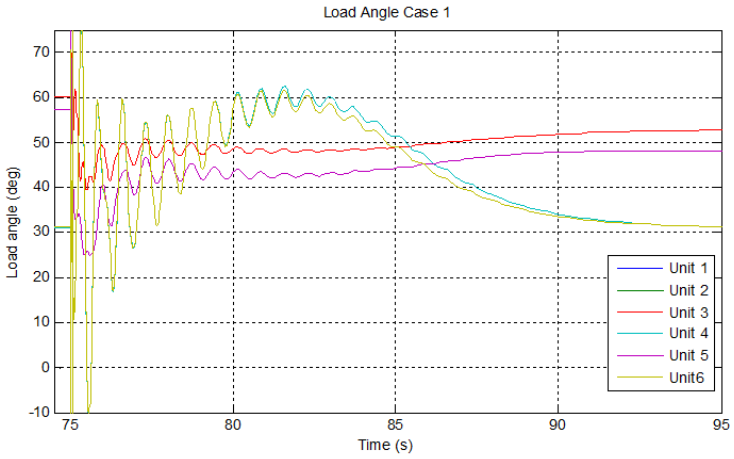

Figure 12: Load Angle CGB Case 1.

5.2.3 Eigenvalues and Eigenvectors.

Table 2 shows the eigenvalues and normalized eigenvectors calculated by Prony Toolbox in Simulink for case 1. The table shows the damping ratio and frequency of oscillation. Additionally, Figure 13 shows the eigenvectors plot. The magnitude of an eigenvector corresponds to the degree of influence for the specific vector to the oscillation, higher magnitude leads to higher oscillation contribution.

Generator	Eigenvalues		Eigenvector		Frequency	Damping	Decay
	σ	ω	Magnitude	Angle (°)	(Hz)	ratio	time (s)
Unit 1	-0.73	9.42	1	0	1.5	0.077	1.37
Unit 2	-0.73	9.42	1	0	1.5	0.077	1.37
Unit 3	-1.8	8.17	0.875	-5	1.3	0.215	0.56
Unit 4	-0.26	9.42	0.875	-1.27	1.5	0.028	3.85
Unit 5	-0.73	9.42	1	0	1.5	0.077	1.37
Unit 6	-0.26	9.42	0.875	-1.27	1.5	0.028	3.85

TABLE 2: Eigenvalues, eigenvectors, frequency and damping ratio for case 1

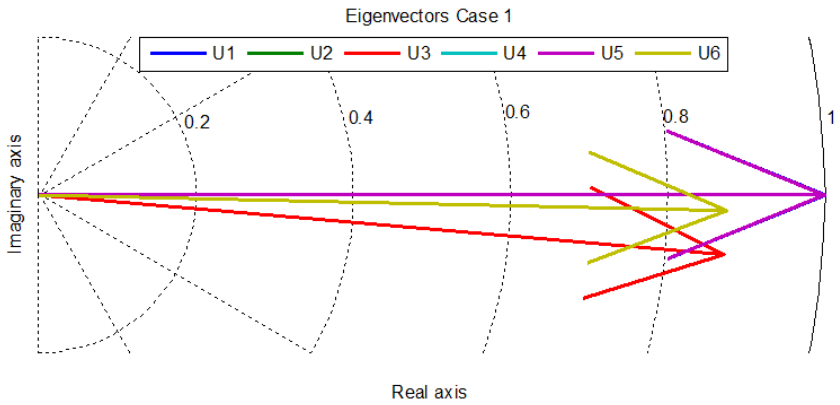

Figure 13: Eigenvectors case 1.

5.3 Case 2 Modelling.

For case 2 modelling have been added a 3-phase short circuit in the transmission line Berlin-San Miguel. There have been including the operation of the circuit breakers in both ends of the line to clean the fault. The fault occurs at 75 seconds and the circuit breakers operate at 75.1 seconds. The total simulation time is 120 seconds.

5.3.1 Rotor Speed

Figure 14 shows the rotor speed during the fault for case 2. It can be seen in the plots that the highest oscillations are for unit 4 and unit 6 again, with a peak value of approximately 1.01 pu. However, the maximum deviation is 0.0123 pu, corresponding to unit 3, but the oscillations are lower for this unit. It takes approximately 5 seconds after the fault occurrence to return to steady state.

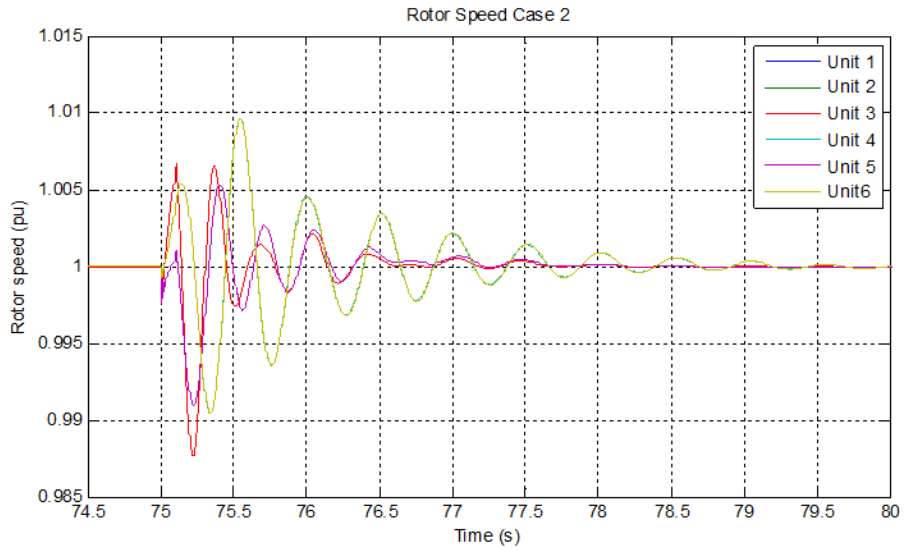

Figure 14: Rotor Speed CGB Case 2.

5.3.2 Load Angle

Figure 15 shows the load angle plot before, during and after the fault. Load angle changes for case 2 are much smaller than for case 1 because the load in the faulted line for this case is lower than the faulted line for case 1.

For unit 1, unit 2 and unit 5 the load angle before the fault is 57.39° and after the fault, for steady state, it changes to 58.22°. For unit 3 the load angle change is for 60.22° to 60.69° and for units 4 and unit 6 the load angle change is for 31.26° to 31.32°.

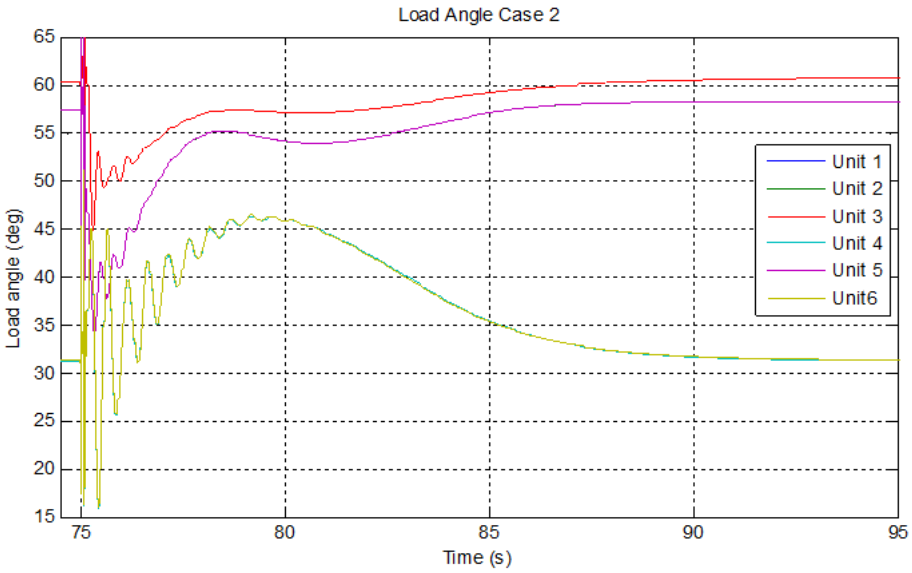

Figure 15: Load Angle CGB Case 2.

5.3.3 Eigenvalues and Eigenvectors.

Table 3 shows the eigenvalues and normalized eigenvectors for case 2 and figure 16 shows the eigenvectors plot. In general, compared with case 1, damping values are bigger, that means that decay time will be smaller. Frequency is very similar for case 2, eigenvectors magnitudes are bigger, eigenvectors angles are very similar and damping ratio are bigger for all units.

Generator	Eigenvalues		Eigenvector		Frequency	Damping	Decay
	σ	ω	Magnitude	Angle (°)	(Hz)	ratio	time (s)
Unit 1	-8.3	10.05	0.821	-0.448	1.6	0.637	0.12
Unit 2	-8.3	10.05	0.821	-0.448	1.6	0.637	0.12
Unit 3	-5.8	13.82	0.615	0.222	2.2	0.387	0.17
Unit 4	-1.6	12.57	1	0	2	0.126	0.63
Unit 5	-8.3	10.05	0.821	-0.448	1.6	0.637	0.12
Unit 6	-1.5	12.57	0.949	0.037	2	0.118	0.67

TABLE 3: Eigenvalues, eigenvectors, frequency and damping ratio for case 2

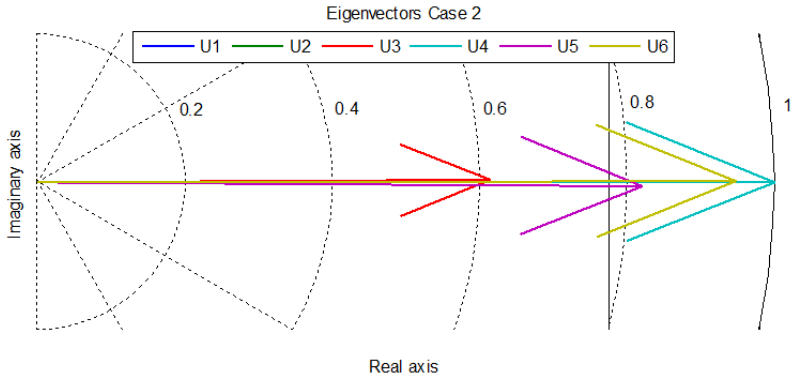

Figure 16: Eigenvectors case 1.

5.4 Case 3 Modelling.

For case 3 modelling the 3-phase short circuit is located in the transmission line 15 de Septiembre-San Miguel. There have been including the operation of the circuit breakers in both ends of the line to clean the fault. The fault occurs at 75 seconds and the circuit breakers operate at 75.1 seconds. The total simulation time is 120 seconds.

5.4.1 Rotor Speed

Figure 17 shows the rotor speed during the fault for case 2. It can be seen in the plots that the highest oscillations are for unit 4 and unit 6 again, with a peak value of approximately 1.008 pu. However, the maximum deviation is 0.0098 pu, corresponding to unit 3, but the oscillations are lower for this unit. It takes approximately 6 seconds after the fault occurrence to return to steady state.

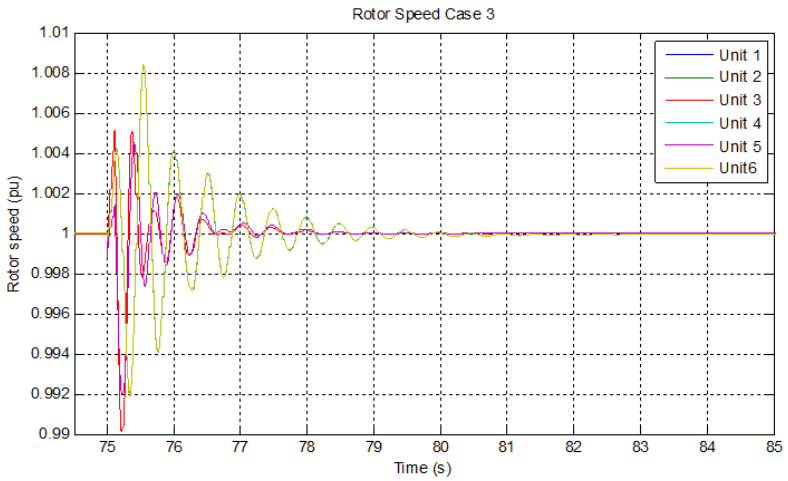

Figure 17: Rotor Speed CGB Case 3.

5.4.2 Load Angle

Figure 18 shows the load angle plot before, during and after the fault. Load angle changes for case 3 are a little higher than case 2 because the load in line 15 de Septiembre-San Miguel is higher than load at line Berlin-San Miguel.

For unit 1, unit 2 and unit 5 the load angle before the fault is 57.39° and after the fault, for steady state, it changes to 55.4°. For unit 3 the load angle change is for 60.22° to 58.52° and for units 4 and unit 6 the load angle change is for 31.26° to 31.33°.

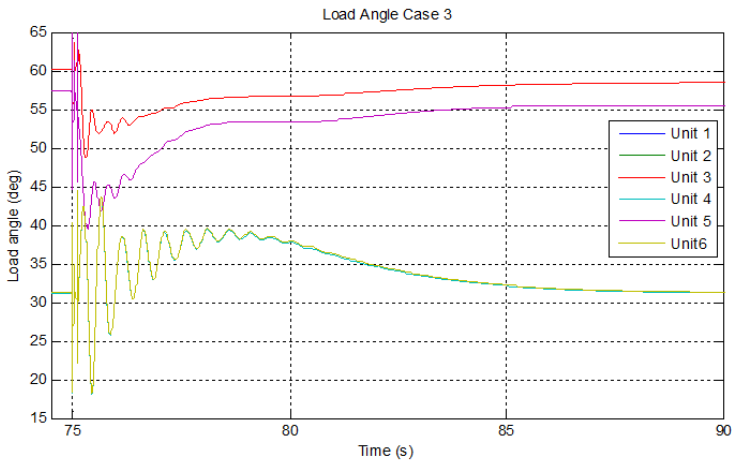

Figure 18: Load Angle CGB Case 3.

5.4.3 Eigenvalues and Eigenvectors.

Table 4 shows the eigenvalues and normalized eigenvectors for case 3 and Figure 19 shows the eigenvectors plot. In general, compared with case 1, damping is smaller for all units except for unit 4 and unit 6. Frequency is bigger for case 3, eigenvectors magnitudes and angles are smaller, damping ratios are very similar for all units except for unit 3.

Generator	Eigenvalues		Eigenvector		Frequency	Damping	Decay
	σ	ω	Magnitude	Angle (°)	(Hz)	ratio	time (s)
Unit 1	-0.37	19.48	0.173	0.038	3.1	0.019	2.7
Unit 2	-0.37	19.48	0.173	0.038	3.1	0.019	2.7
Unit 3	-1.2	18.85	0.182	0.023	3	0.064	0.83
Unit 4	-1.5	18.85	1	0	3	0.079	0.67
Unit 5	-0.37	19.48	0.173	0.038	3.1	0.019	2.7
Unit 6	-1.3	18.85	1	0	3	0.069	0.77

TABLE 4: Eigenvalues, eigenvectors, frequency and damping ratio for case 3

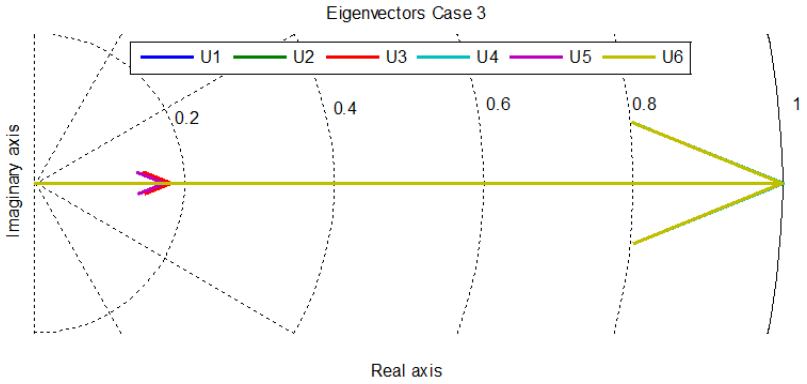

Figure 19: Eigenvectors case 3.

6. CONCLUSIONS

This project presents a flexible model of the CGB and the surrounding grid, and it can be extended to add more units in the surroundings to make dynamics studies. The models are more flexible than other software like PSSE, where made changes in parameters or inclusive the model is more complicated.

Eigenvectors plots show that the oscillation mode for our case of study is local mode or Machine system mode because all the units of CGB swing together with respect to the rest of the power system. By extending the model (i.e. including more of the surrounding grid and other power plants) we assume that we would get additional oscillation modes, such as inter-area modes. The developed model is, however, very well suited for studying local phenomena.

During the transient period, when the configuration of the system changes, the system seeks to regain stability at a new operation point, causing changes in load angles of the generators.

There is an inverse relation between damping values and damping ratio, as the highest damping values, lowest damping ratio. It means that for a low damping value the rate of decay of the amplitude of the oscillation (damping ratio) will be low too, giving a high decay time for the oscillation.

The case that has the worst effect in terms of power system stability is when the short circuit is located in the line Berlin-15 de Septiembre, that correspond to case 1, and will be taken as the reference for comparison effects.

Transmission line Berlin-15 de Septiembre is more loaded that the others transmission lines part of this study, this condition causes that the effect of the SC in the stability of the system was worst for these cases.

Case 2 has the highest damping ratio than case 1. It means that time to decay to 37% of the initial amplitude of oscillation will be smaller for all unit in case 2. On the other hand, case 3 has the smallest damping ratio for unit 1, unit 2, unit 3 and unit 5. It means that unit 4 and unit 6 have the lowest decay time despite having the highest oscillation magnitudes.

The units with the smallest damping ratio are unit 4 and unit 6 in all cases; it means that for these units, decay time to reach stable state again is bigger compared with all the other units. Unit 4 and unit 6 have the highest degree of influence on oscillation too because they have the highest eigenvector magnitude for all cases.

All cases present big oscillations during the fault occurrence and tend to steady state after the circuit breakers operation. After reaching steady state again, there have been changes in load angles, been the biggest one of 9.18° for unit 1, unit 2 and unit 5 in case 1. But, for unit 4 and unit 6 there have been not changes practically. This is because of unit 4 and unit 6 return to the pre-fault operation point in the post fault period. The rest of the unit change operation point from Pre-fault to Post-fault condition, as described in 3.2.

Loss of the transmission line causes a small change in load angle because of change in impedances of the network, but the biggest influence in load angle is because of change of operating point for unit 1, unit 2, unit 3 and unit 5. There are practically non changed in load angles for unit 4 and unit 6, related basically with changes in the impedances of the network caused by loss of transmission line or load changes.

REFERENCES

Bertani, R., 2010: Geothermal power generation in the world. 2005-2010 update report. *World Geothermal Congress 2010*, Bali, Indonesia, April 25-30, 2010.

ETESAL, 2015: *Transmission system data base 2015*. Empresa Transmisora de El Salvador, S.A. de C.V.

Fridleifsson, I.B., and Haraldsson, I.G., 2011: Geothermal energy in the world with special reference to Central America. *Short Course of Geothermal Drilling, Resource Development and power plants*, Organized by UNU-GTP and LaGeo in Santa Tecla, El Salvador, January 16-22, 2011.

Guidos, J., and Burgos, J., 2012: Geothermal Activity and Development in El Salvador-Producing and developing. *Short course on Geothermal development and Geothermal Wells*, Organized by UNU-GTP and LaGeo, in Santa Tecla, El Salvador, March 11-17, 2012.

Hauer, J.F., Demeure, C.J., Scharf, L.L., 1990: *Initial results in prony analysis of power system response signals*. IEEE Transactions on Power Systems, Vol. 5, No. 1, February 1990.

IEEE, 1992: IEEE Recommended Practice for Excitation System Models for Power System Stability Studies. IEEE Std 421.5-1992.

Kundur, P., 1994: *Power system Stability and control.* McGraw-Hill, Inc. 1197 pp.

Kundur et al., 2003: *Definition and classification of power system stability*. IEEE/CIGRE Joint Task Force on Stability Terms and Definitions.

SIEMENS, 2012: PSS®E 33.2 Program application guide. July, 2012.

SIGET, 2017: Boletín de estadísticas eléctricas N° 19 año 2017. SIGET, San Salvador.

UT, 2013: *Technical data base 2013*. Unidad de Transacciones S.A. de C.V., www.ut.com.sv